

Supplementary information:

Vernoux et al.

The auxin signalling network translates dynamic input into robust patterning at the shoot apex

Table of contents

1- Supplementary Figures 1-9

2- Supplementary Tables 1-3

See separate file for Supplementary Table 1: SuppTable1.xls (Results of the yeast two-hybrid analysis)

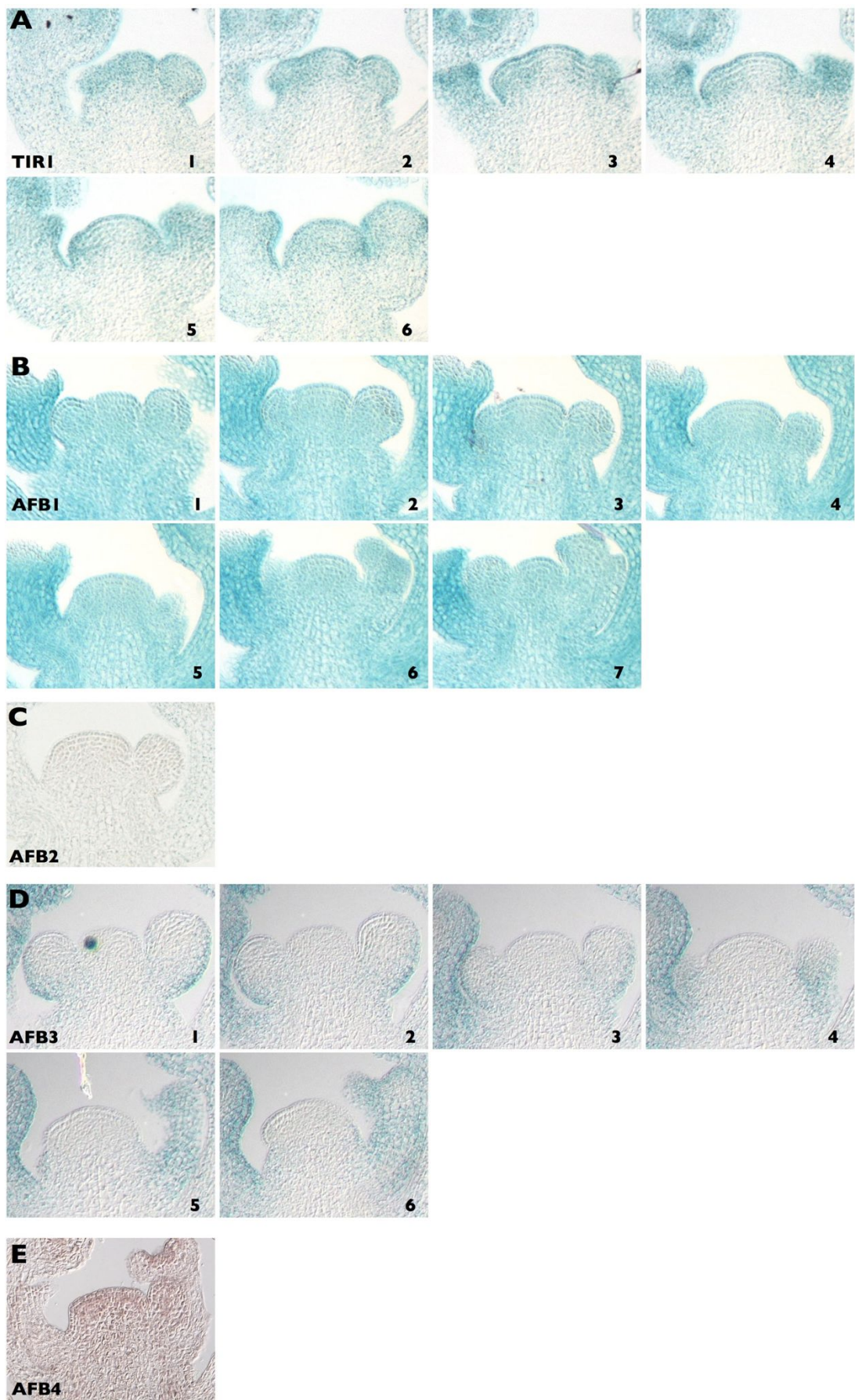
3- Supplementary text: Model of the ARF-Aux/IAA signalling network

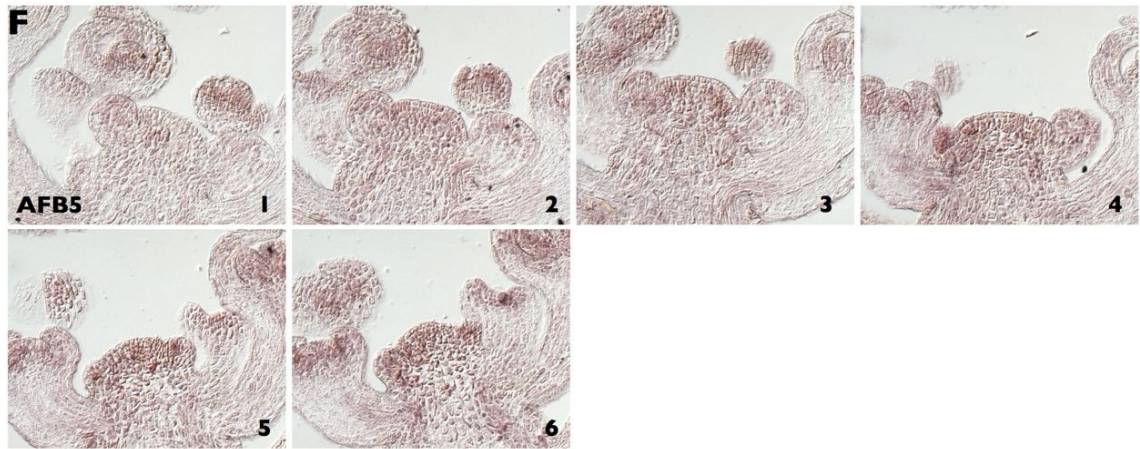
See separate file: NoteS1.pdf

4- SBML version of the ARF-Aux/IAA signalling model

See separate file: AuxinSignalingODEmodel.xml

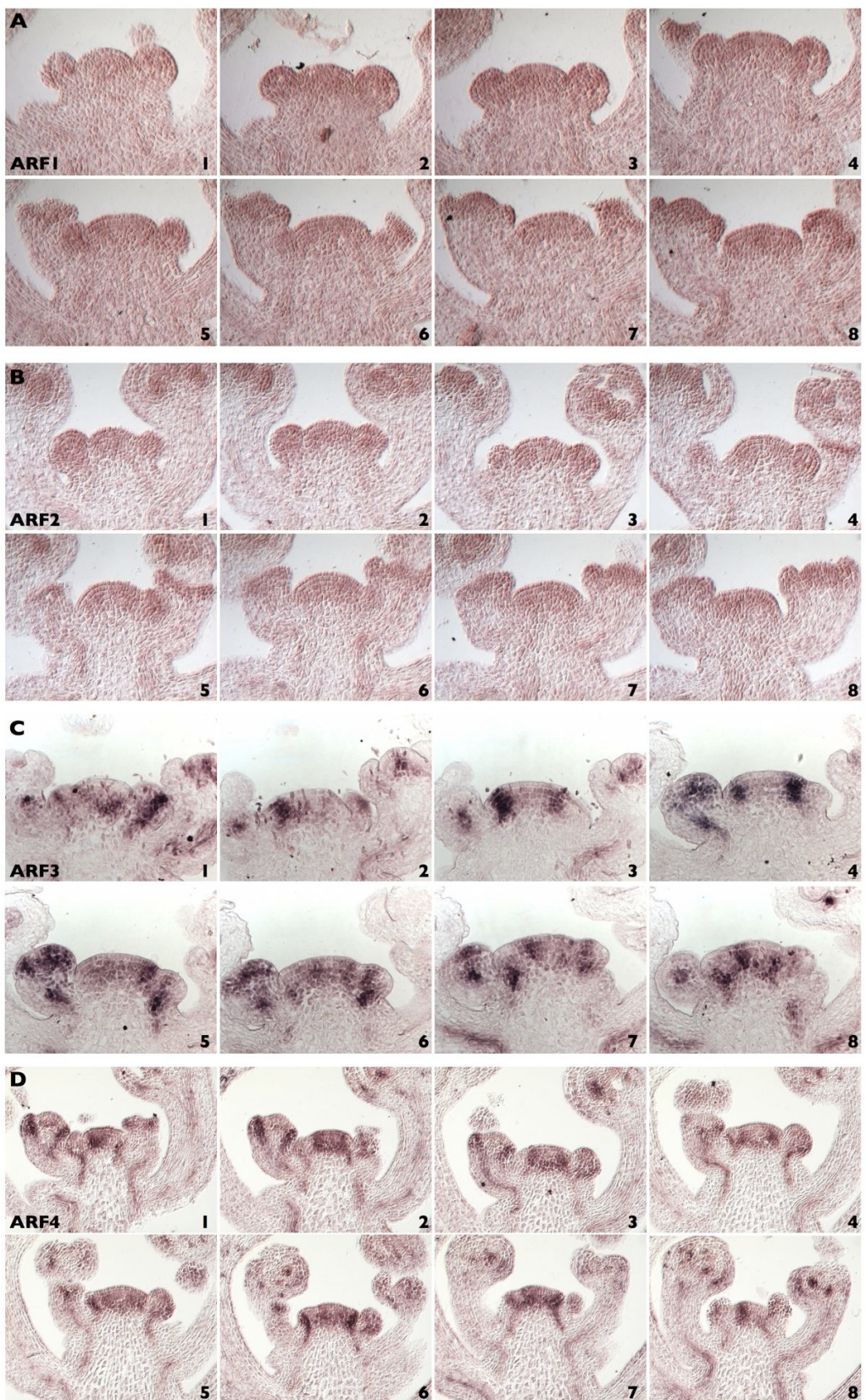
5- Supplementary References

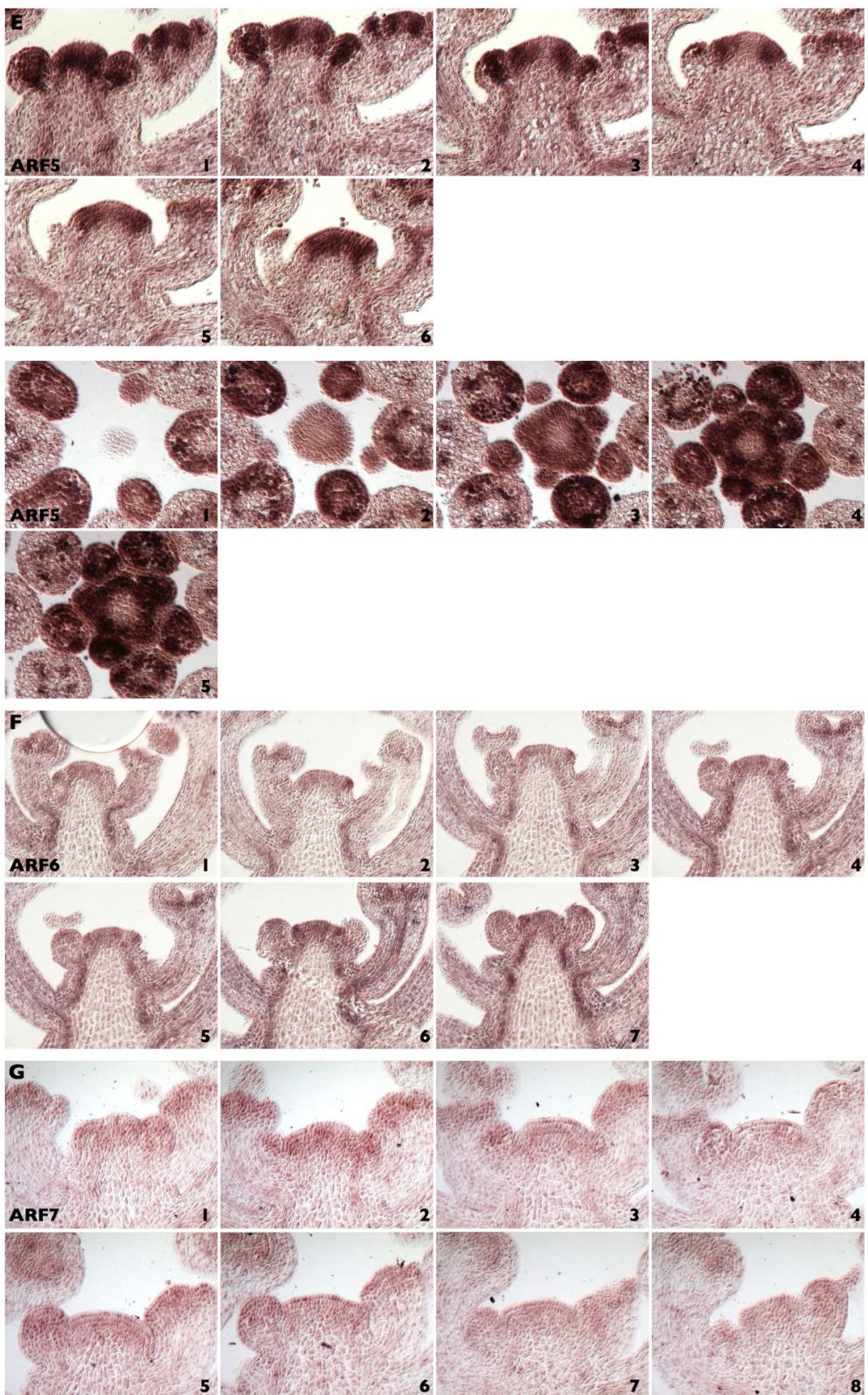


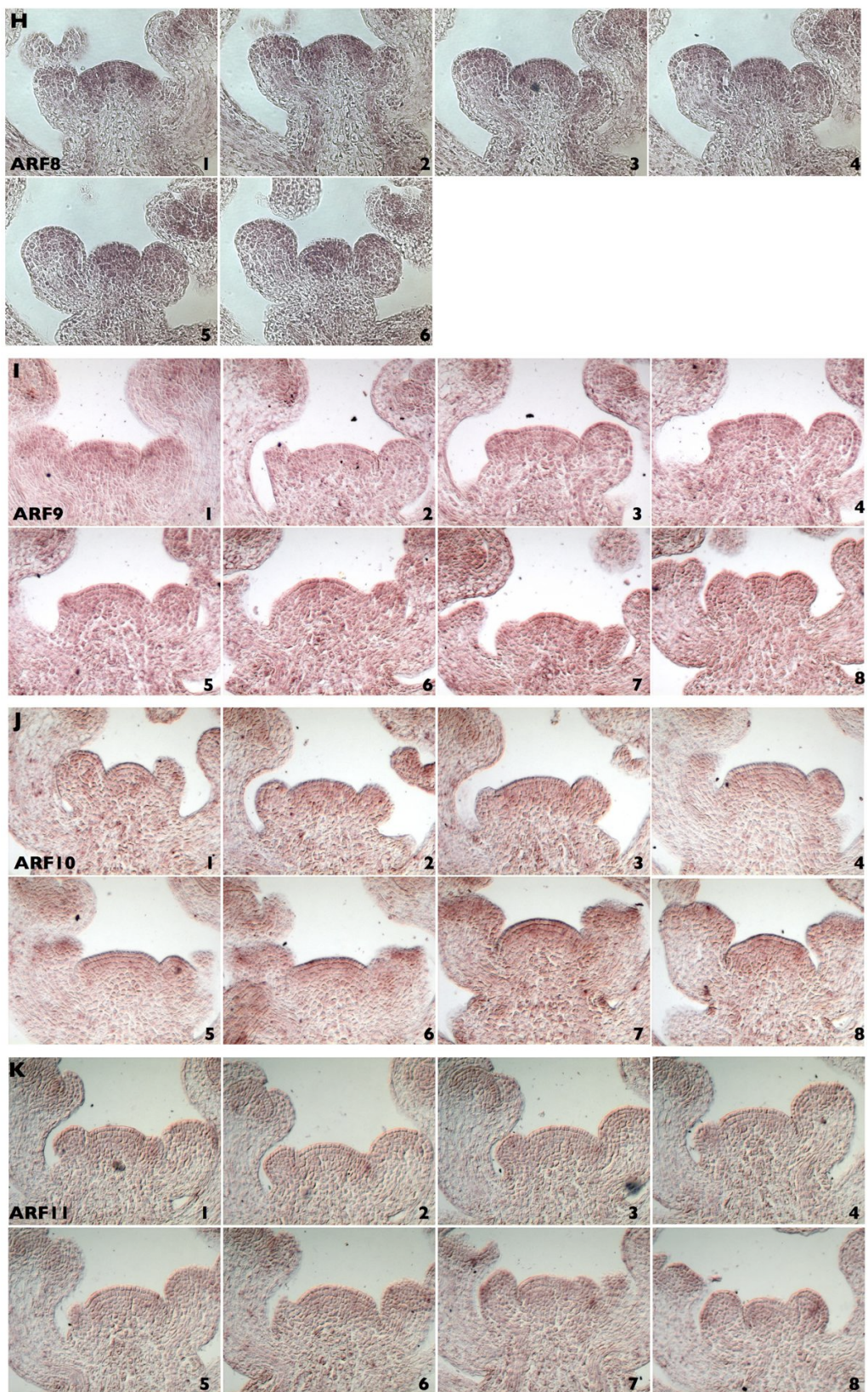


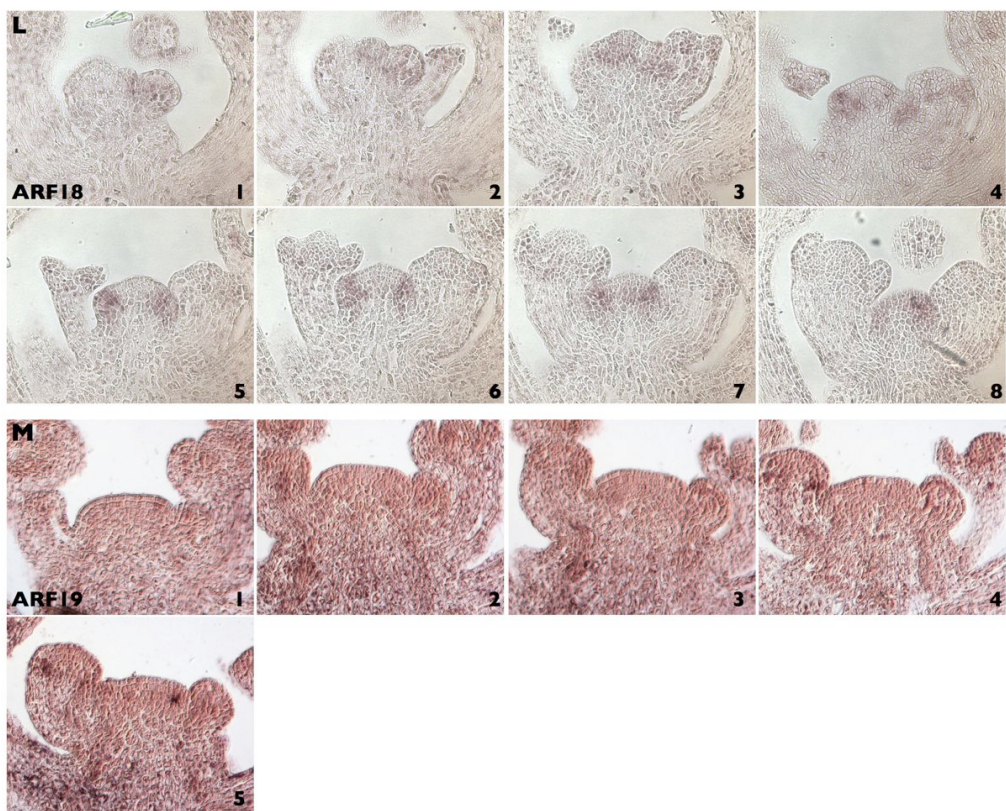
Supplementary Figure 1. TIR1/AFB expression patterns in the inflorescence meristem.

Serial sections showing expression of TIR1/AFB proteins fused to GUS (A-D) or *AFB4/5* mRNA as visualized by RNA *in situ* hybridization (E,F). The name of the gene is indicated on the figure. Scale is identical in all images for each serial section.



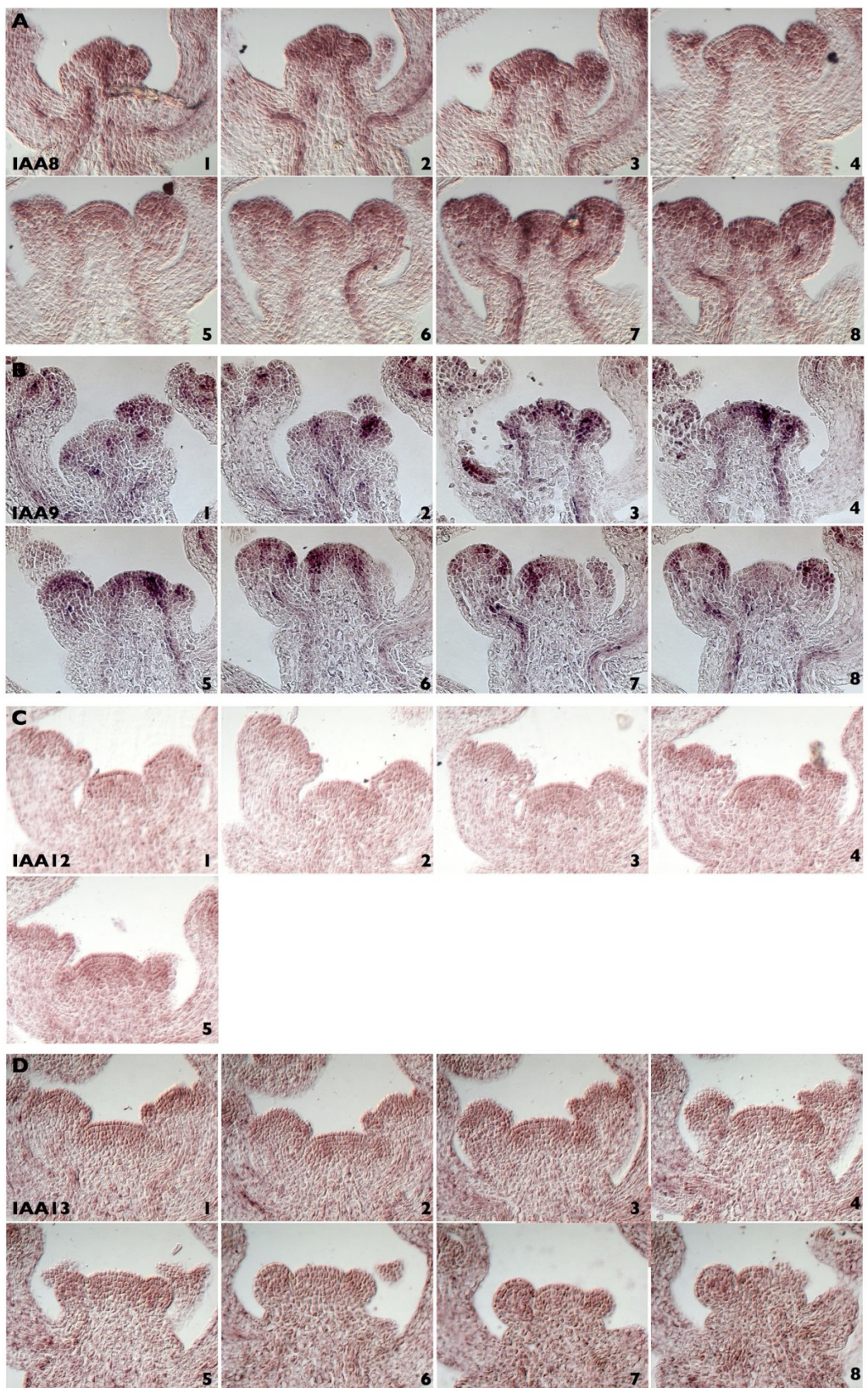


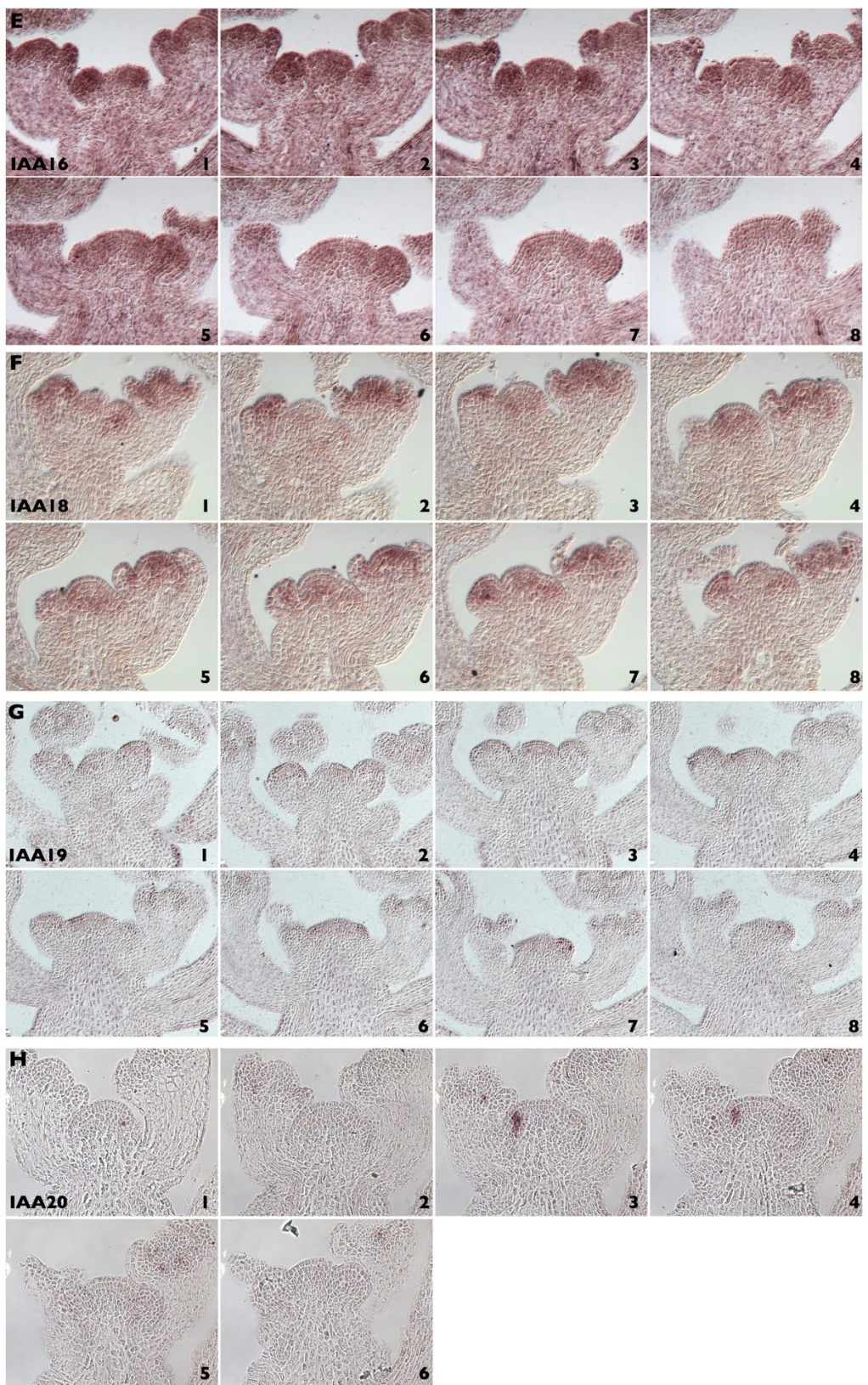


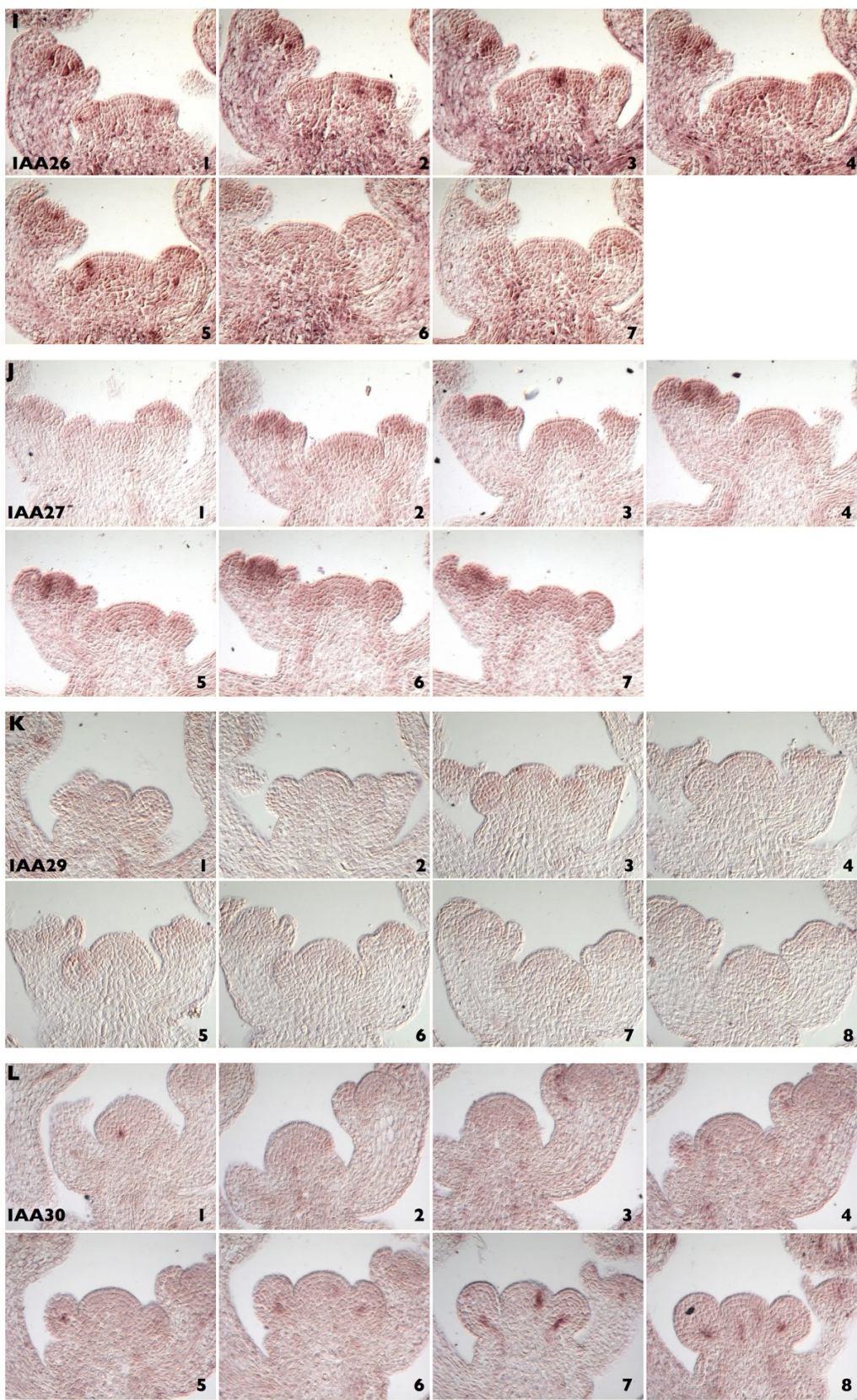


Supplementary Figure 2. ARF expression patterns in the inflorescence meristem.

(A-M) Serial sections showing expression of *ARF* genes as visualized by RNA *in situ* hybridization. The name of the gene is indicated on the figure. Scale is identical in all images for each serial section.

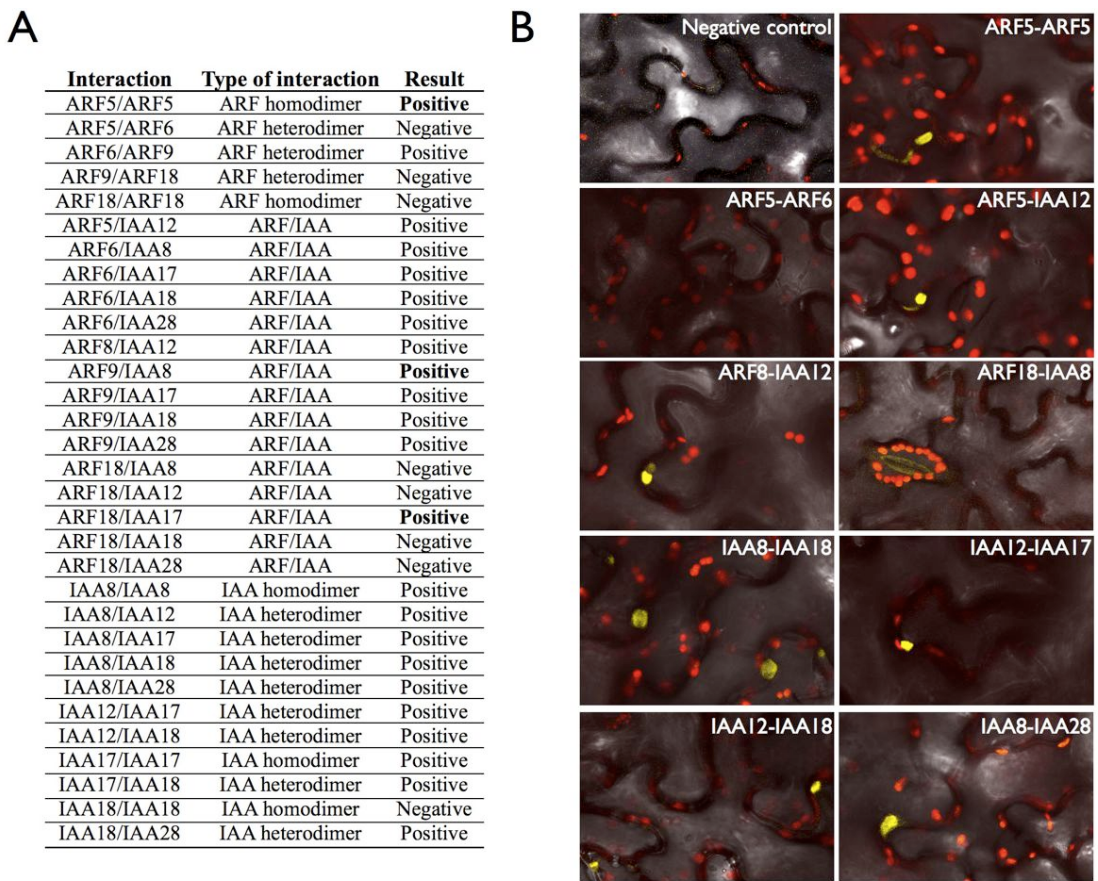






Supplementary Figure 3. Aux/IAA expression patterns in the inflorescence meristem.

(A-L) Serial sections showing expression of *Aux/IAA* genes as visualized by RNA *in situ* hybridization. The name of the gene is indicated in the figure. For each serial section, scale is identical in all images.



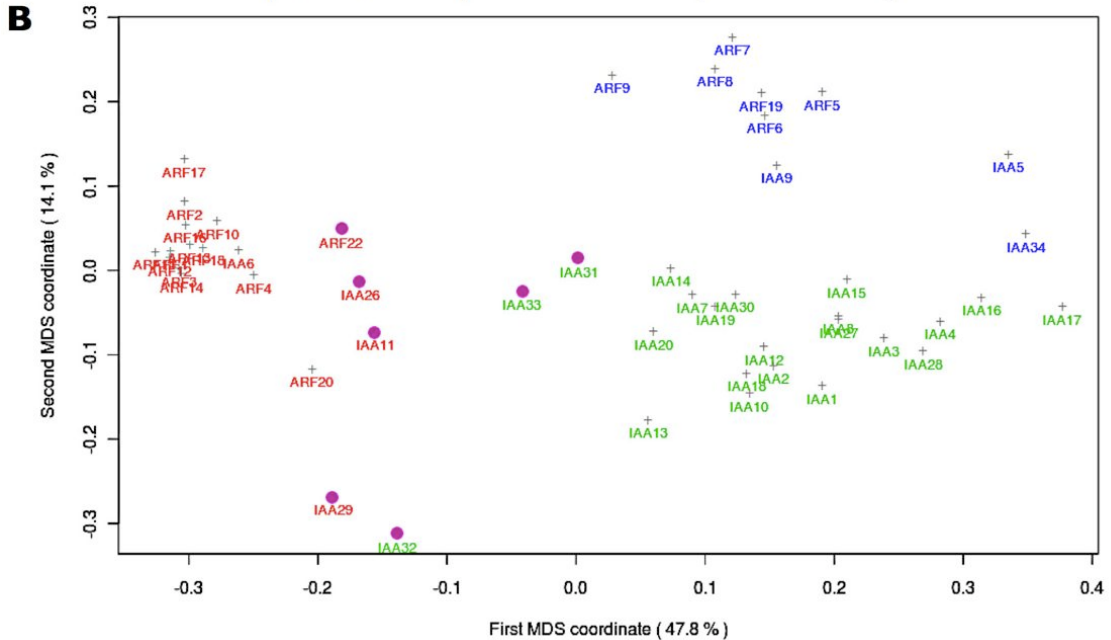
Supplementary Figure 4. *In planta* analysis of Aux/IAA-ARF interactions.

Bimolecular Fluorescence complementation (BiFC) was used to test 31 Aux/IAA-ARF interactions *in planta*. The set of interactions included both positive and negative interactions as predicted from the Y2H interactome analysis. (A) Summary of the results of the BiFC analysis. All the results were coherent with the results from the Y2H analysis except for 3 interactions (result indicated in bold). (B) Confocal images for a selection of the tested interactions showing results of BiFC in *Nicotiana Benthamina* leaves. Yellow: YFP; Red: autofluorescence; Grey levels: transmission channel. Scale is identical in all images.

A

cluster I (22 proteins): IAA3, IAA8, IAA18, IAA2, IAA4, IAA1, IAA16, IAA10, IAA13, IAA28, IAA15, IAA12, IAA27, IAA19, IAA14, IAA17, IAA20, IAA30, IAA7, IAA31, IAA33, IAA32.
cluster II (9 proteins): ARF5, ARF19, ARF8, ARF7, ARF6, IAA5, ARF9, IAA9, IAA34.
cluster III (18 proteins): ARF11, ARF14, ARF3, ARF1, ARF13, IAA6, ARF4, ARF18, ARF16, ARF17, ARF10, ARF2, ARF12, ARF20, ARF22, IAA1, IAA29, IAA26.

$$\hat{\Pi} = \begin{bmatrix} 0.68 & 0.87 & 0.11 \\ 0.87 & 0.34 & 0.21 \\ 0.11 & 0.21 & 0.04 \end{bmatrix} \quad D = \begin{bmatrix} 0.29 & 0.36 & 0.47 \\ 0.36 & 0.25 & 0.50 \\ 0.47 & 0.50 & 0.16 \end{bmatrix}$$



Supplementary Figure 5. Cluster analysis of the global Aux/IAA-ARF interactome using MixNet.

(A) Results of the MixNet algorithm for the global interactome. We applied the MixNet algorithm to the ARF-Aux/IAA protein network for $Q = 2$ to 10 clusters. The model selection criterion favours 4 clusters. Since this model selection criterion is only asymptotically valid (i.e. for large N), this number of clusters should only be considered as indicative in our case and we thus explored neighbouring solutions. The results are presented for $Q = 3$ clusters. The proteins are ordered from the most to the least central in each cluster based on the distance of the protein to the cluster ($D(i,q)$; data not shown). The connectivity probability matrix $\hat{\Pi}$ and the cluster distance matrix $\{D(q,\ell)\}_{q,\ell=1,\dots,Q}$ are given. The three clusters differ strongly in terms of connectivity profiles; compare the rows of matrix $\hat{\Pi}$. The three clusters are also well separated; compare the diagonal elements of the cluster distance matrix $\{D(q,\ell)\}$.

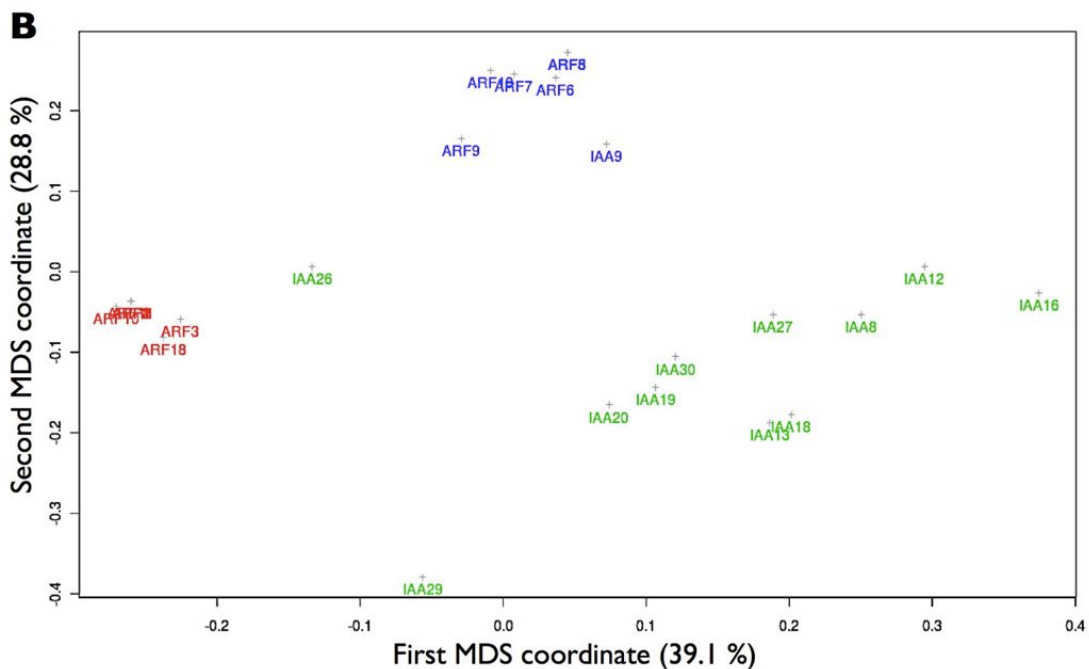
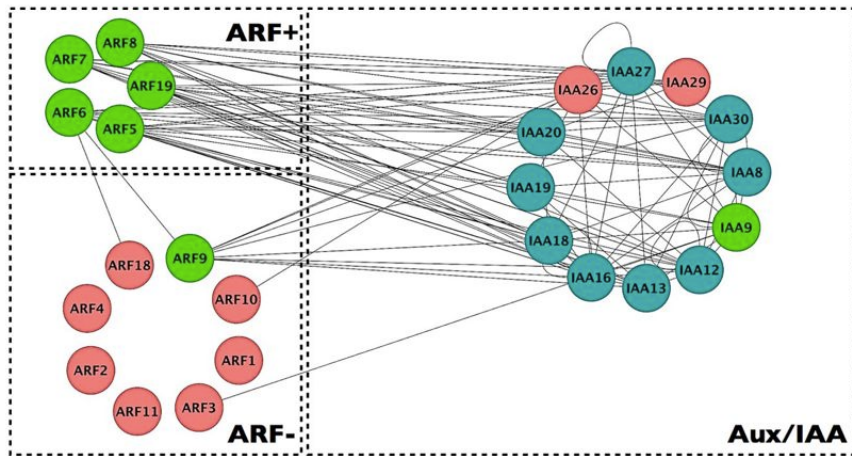
corresponding to within-cluster distances to the off-diagonal elements corresponding to between-cluster distances. The proteins in italics form the fourth cluster when the MixNet algorithm is applied for $Q = 4$ clusters. In this case, the 3 most peripheral proteins of cluster I are grouped with the 4 most peripheral proteins of cluster II to form a second Aux/IAA cluster. This fourth cluster is not well defined (the within-cluster distance $D(\text{IV},\text{IV}) = 0.34$ is larger than the between-cluster distance $D(\text{III},\text{IV}) = 0.3$ (data not shown), indicating that the 3-cluster solution is the most adequate. (B) Visualization of the clusters using MDS. The first two MDS coordinates were deduced from the pairwise distances between proteins $\{D(i,j) | i, j = 1, \dots, N\}$. These first two coordinates account for 61.9 % of the total variation. The proteins from cluster I, II and III are figured in green, blue and red respectively. Note that the clusters are compact (except for a few outliers) and well separated. The proteins that are in the 4th cluster when the MixNet algorithm is applied for $Q = 4$ are found amongst the outliers (labelled in purple).

A

cluster I (11 proteins): IAA18, IAA13, IAA16, IAA8, IAA12, IAA27, IAA19, IAA20, IAA29, IAA30, IAA26.

cluster II (7 proteins): ARF5, ARF8, ARF7, ARF19, ARF9, ARF6, IAA9.

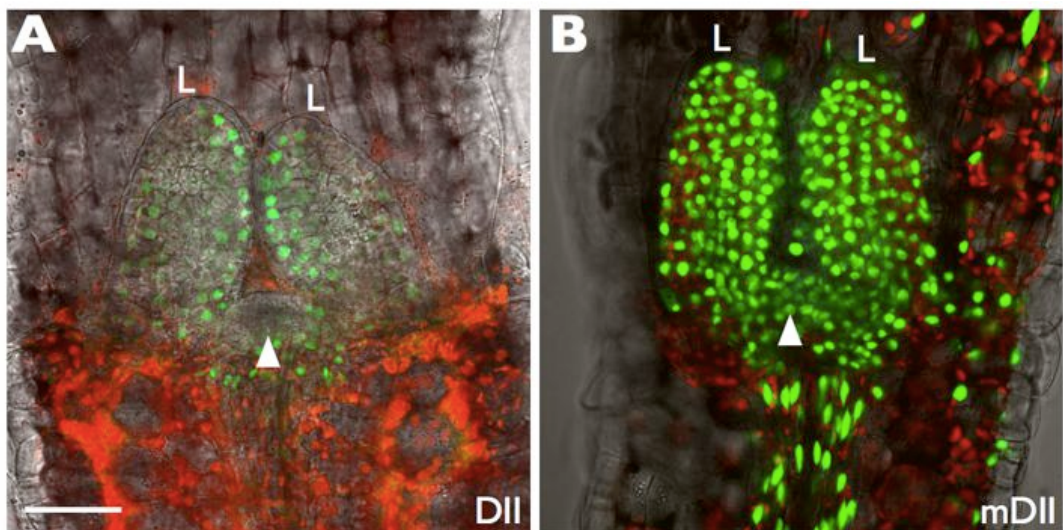
cluster III (7 proteins): ARF1, ARF2, ARF4, ARF11, ARF3, ARF10, ARF18



Supplementary Figure 6. Cluster analysis of the meristem Aux/IAA-ARF interactome using MixNet.

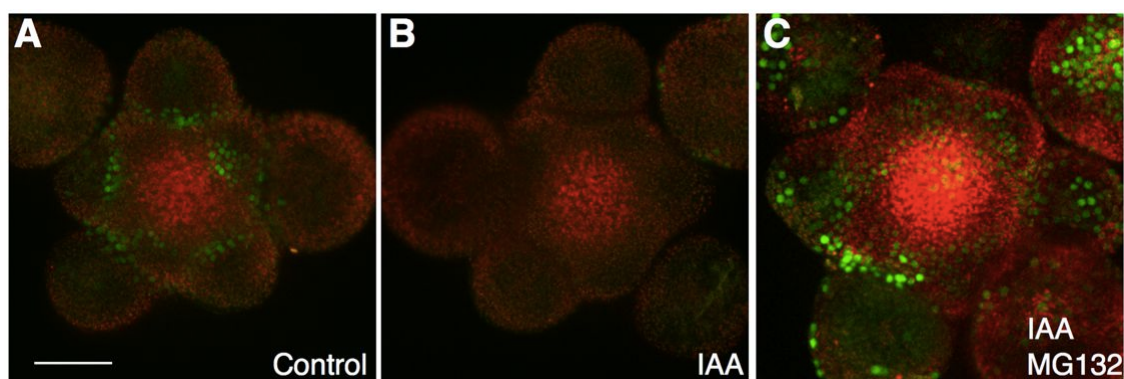
(A) Results of the MixNet analysis for the SAM interactome. We applied the MixNet algorithm to the SAM subnetwork for $Q = 3$ clusters. The three clusters obtained are almost nested in the three clusters obtained for the complete network, the only exceptions being IAA29 and IAA26, peripheral in cluster III, which are then assigned to cluster I with almost all the other Aux/IAAs. As in the case of the complete network, the

proteins are ordered from the most to the least central in each cluster based on the distance of the protein to the cluster ($D(i,q)$; data not shown) (A). A graphic representation of the structure of the network using Cytoscape (www.cytoscape.org) is given. The Aux/IAA, ARF activator (ARF+) and repressors (ARF-) have been grouped. The vertices are colored according to their MixNet cluster: blue for cluster I, green for cluster II and pink for cluster III. (B) Visualization of the clusters using MDS. The first two MDS coordinates were deduced from the pairwise distances between proteins $\{D(i,j)\}_{i,j=1,\dots,N}$ and explain 67.9% of the total variation. The proteins assigned to cluster I, II and III are figured in green, blue and red respectively. Note again that the clusters are compact (except for a few outliers) and well separated.



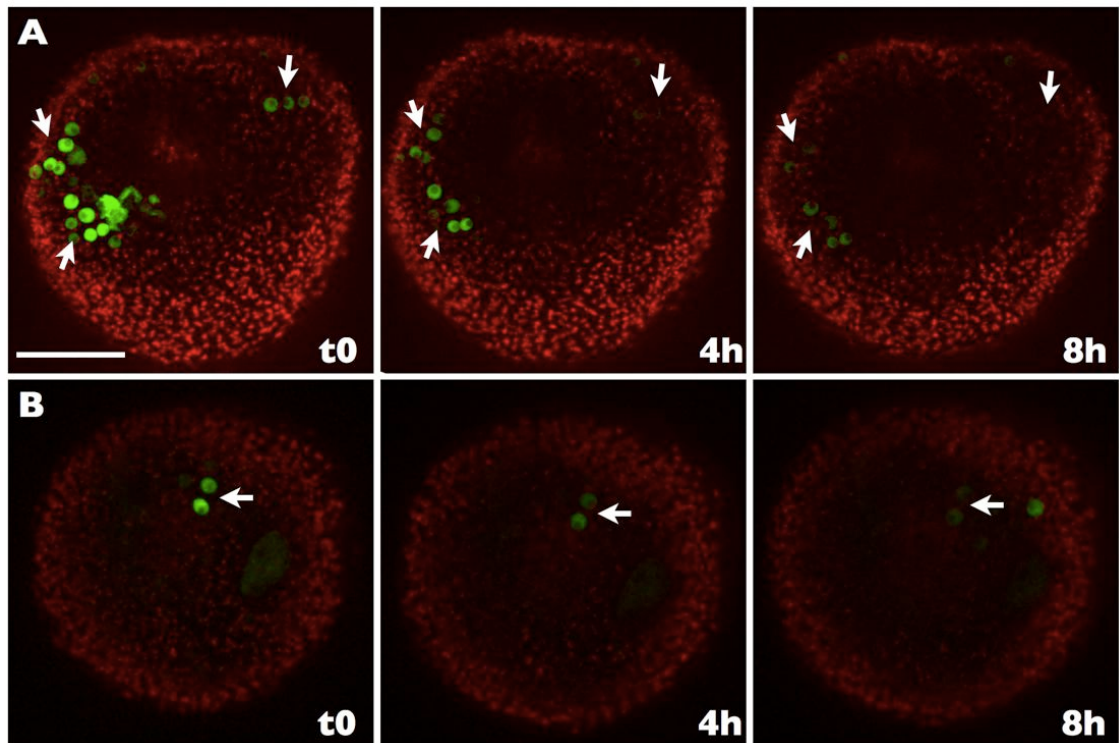
Supplementary Figure 7. Distribution of DII-VENUS and mDII-VENUS in vegetative shoot meristem.

DII-VENUS (A) and mDII-VENUS (B) expression was analyzed in 5 day old plantlets using confocal microscopy. VENUS fluorescence is in green. The red channel visualizes auto-fluorescence. One cotyledon has been peeled out to reveal the meristem (arrowhead). The two first leaves (L) are indicated. Note the absence of DII-VENUS signal at the centre of the meristem and the homogenous distribution of mDII-VENUS. Scale is identical in (A,B). Scale bar: 40 μ m.



Supplementary Figure 8. Proteasome inhibitors interfere with DII-VENUS auxin-induced degradation in the SAM.

Images were obtained by confocal microscopy. DII-VENUS is in green. The red channel visualizes auto-fluorescence in the inflorescence meristem. All the images were taken using the same settings. Plants were treated either with DMSO (control; A), 1 μ M IAA (B) or co-treated with IAA and the MG132 proteasome inhibitor (C). Note that the degradation of DII-VENUS induced by auxin is largely blocked by MG132. Scale is the same in (A-C). Scale bar: 40 μ m.



Supplementary Figure 9. Instability of VENUS visualized in *DR5::VENUS* plants upon chemical inhibition of auxin transport.

To verify that the stability of DR5::VENUS fluorescence observed in inflorescence meristem was not solely due to the stability of the VENUS protein, we germinated DR5::VENUS plants on the auxin transport inhibitor NPA to generate pin-like inflorescences *in vitro*. The plant were then transferred on a new NPA-free medium and DR5::VENUS expression was followed over time as described (Hamant *et al*, 2008). Due to the perturbation of auxin transport, we often observed in these conditions transient peaks of DR5::VENUS expression that were not followed by organ induction. Representative results from 2 independent time-courses are shown (A,B). Arrows indicates group of nuclei showing rapid decrease in fluorescence. Note that in each cases drastic diminution in VENUS fluorescence could be observed after 4 hours, suggesting a half-life for the protein in that time range. Scale is identical in all images. Scale bar: 20 μ m.

Supplementary Table 2. Summary of Aux/IAA-ARF interactions tested in the literature.

Interaction	Results	Method used	References	Full interactome data
IAA1/IAA1	positive	Y2H / His3 - LacZ	(1)	positive
IAA1/IAA1	positive	Y2H / LacZ	(2)	
IAA1/IAA2	positive	Y2H / His3 - LacZ	(1)	positive
IAA1/IAA3	positive	Y2H / His3 - LacZ	(1)	positive
IAA1/IAA4	positive	Y2H / His3 - LacZ	(1)	positive
IAA1/IAA8	positive	Y2H / His3 - LacZ	(1)	positive
IAA1/IAA9	positive	Y2H / His3 - LacZ	(1)	positive
IAA1/IAA16	positive	Y2H / His3 - LacZ	(1)	positive
IAA1/IAA17	positive	Y2H / His3 - LacZ	(1)	positive
IAA1/IAA18	positive	Y2H / His3 - LacZ	(1)	positive
IAA1/IAA19	positive	Y2H / His3 - LacZ	(1)	positive
IAA1/IAA20	positive	Y2H / His3 - LacZ	(1)	negative
IAA2/IAA2	positive	Y2H / His3 - LacZ	(1)	positive
IAA3/IAA17	positive	Y2H / LacZ	(3)	positive
IAA6/IAA6	positive	Y2H / LacZ	(2)	negative
IAA12/IAA12	positive	Y2H / LacZ	(4)	positive
IAA12/IAA12	positive	BiFC	(5)	
IAA13/IAA13	positive	Y2H / LacZ	(2)	positive
IAA17/IAA17	positive	Y2H / LacZ	(3)	positive
IAA19/IAA19	positive	Y2H / LacZ	(2)	
IAA19/IAA19	~20% dimerization ¹	FCCS	(6)	positive
ARF1/ARF1	positive ²	Y2H / LacZ	(3)	negative
ARF5/ARF1	positive ²	Y2H / LacZ	(3)	negative*
ARF5/ARF1	negative	Y2H / LacZ	(7)	
ARF5/ARF2	negative	Y2H / LacZ	(7)	negative
ARF5/ARF4	negative	Y2H / LacZ	(7)	negative
ARF5/ARF5	positive ²	Y2H / LacZ	(7)	
ARF5/ARF5	positive ²	Y2H / LacZ	(2)	negative*
ARF5/ARF5	No association	FCCS	(6)	
ARF5/ARF6	negative	Y2H / LacZ	(7)	negative
ARF5/ARF7	positive	Y2H / LacZ	(7)	negative*
ARF5/ARF7	< 20% dimerization ³	FCCS	(6)	
ARF5/ARF8	negative	Y2H / LacZ	(7)	negative
ARF5/ARF9	negative	Y2H / LacZ	(7)	negative
ARF5/ARF11	negative	Y2H / LacZ	(7)	negative
ARF7/ARF1	negative	Y2H / LacZ	(7)	negative
ARF7/ARF2	negative	Y2H / LacZ	(7)	negative
ARF7/ARF4	negative	Y2H / LacZ	(7)	negative
ARF7/ARF6	positive	Y2H / LacZ	(7)	negative

ARF7/ARF7	positive	Y2H / LacZ	(7)	
ARF7/ARF7	< 20% dimerization ³	FCCS	(6)	negative*
ARF7/ARF7	positive ²	Y2H / LacZ	(2)	
ARF7/ARF8	positive ²	Y2H / LacZ	(7)	negative
ARF7/ARF9	negative	Y2H / LacZ	(7)	negative
ARF7/ARF11	negative	Y2H / LacZ	(7)	negative
ARF8/ARF8	negative	Y2H / LacZ	(2)	negative
ARF1/IAA12	positive	Y2H / LacZ	(8)	negative
ARF1/IAA13	positive	Y2H / LacZ	(8)	negative
ARF1/IAA17	positive	Y2H / LacZ	(3)	negative
ARF5/IAA1	positive	Y2H / LacZ	(2)	positive
ARF5/IAA3	positive	Y2H / LacZ	(9)	positive
ARF5/IAA6	positive	Y2H / LacZ	(2)	negative
ARF5/IAA12	positive	Y2H / LacZ	(4)	
ARF5/IAA12	positive	Y2H / LacZ	(7)	positive
ARF5/IAA12	positive	Y2H / LacZ	(9)	
ARF5/IAA12	positive	BiFC	(5)	
ARF5/IAA13	positive	Y2H / LacZ	(2)	positive
ARF5/IAA14	positive	Y2H / LacZ	(10)	positive
ARF5/IAA17	positive	Y2H / LacZ	(3)	positive
ARF5/IAA19	positive	Y2H / LacZ	(2)	positive
ARF5/IAA19	100% dimerization	FCCS	(6)	
ARF6/IAA1	positive	Y2H / His3 - LacZ	(1)	positive
ARF7/IAA1	positive	Y2H / His3 - LacZ	(1)	positive
ARF7/IAA1	positive	Y2H / LacZ	(2)	
ARF7/IAA6	positive	Y2H / LacZ	(2)	negative
ARF7/IAA12	positive	Y2H / LacZ	(7)	positive
ARF7/IAA13	positive	Y2H / LacZ	(2)	positive
ARF7/IAA14	positive	Y2H / LacZ	(10)	positive
ARF7/IAA18	positive	Y2H / LacZ	(11)	positive
ARF7/IAA19	positive	Y2H / LacZ	(2)	
ARF7/IAA19	positive	Pull-down	(2)	positive
ARF7/IAA19	100% dimerization	FCCS	(6)	
ARF8/IAA1	positive	Y2H / LacZ	(2)	positive
ARF8/IAA6	positive	Y2H / LacZ	(2)	negative
ARF8/IAA13	positive	Y2H / LacZ	(2)	positive
ARF8/IAA19	positive	Y2H / LacZ	(2)	positive
ARF11/IAA1	positive	Y2H / His3 - LacZ	(1)	negative
ARF19/IAA3	positive	Y2H / LacZ	(9)	positive
ARF19/IAA12	positive	Y2H / LacZ	(9)	positive
ARF19/IAA14	positive	Y2H / LacZ	(10)	positive
ARF19/IAA18	positive	Y2H / LacZ	(11)	positive

The method used to test the interactions is indicated along with the reporter systems for yeast two-hybrid (Y2H). Divergent interaction results in the full interactome analysis are indicated in bold and * indicates divergent results in the literature. ¹ Statistically different from all controls; ² Low LacZ activity; ³ Not statistically different from all controls.

1. J. Kim, K. Harter, A. Theologis, *Proc Natl Acad Sci U S A* **94**, 11786 (Oct 28, 1997).
2. K. Tatematsu *et al.*, *Plant Cell* **16**, 379 (Feb, 2004).
3. F. Ouellet, P. J. Overvoorde, A. Theologis, *Plant Cell* **13**, 829 (Apr, 2001).
4. T. Hamann, E. Benkova, I. Baurle, M. Kientz, G. Jurgens, *Genes Dev* **16**, 1610 (Jul 1, 2002).
5. H. Szemenyei, M. Hannon, J. A. Long, *Science* **319**, 1384 (Mar 7, 2008).
6. H. Muto *et al.*, *Plant Cell Physiol* **47**, 1095 (Aug, 2006).
7. C. S. Hardtke *et al.*, *Development* **131**, 1089 (Mar, 2004).
8. T. Ulmasov, J. Murfett, G. Hagen, T. J. Guilfoyle, *Plant Cell* **9**, 1963 (Nov, 1997).
9. D. Weijers *et al.*, *EMBO J* **24**, 1874 (May 18, 2005).
10. H. Fukaki, Y. Nakao, Y. Okushima, A. Theologis, M. Tasaka, *Plant J* **44**, 382 (Nov, 2005).
11. T. Uehara, Y. Okushima, T. Mimura, M. Tasaka, H. Fukaki, *Plant Cell Physiol* **49**, 1025 (Jul, 2008).

Supplementary Table 3: Oligonucleotides used in this study.

RT-qPCR		
Targets /names	Forward	Reverse
ARF8	5'TGGCAGCTGTATTCGTTGA3'	5'CCAAACGTTATTCACAAATGACTC3'
IAA29	5'CCGAGTCTTCATAGTTACGATG3'	5'CGAACATGACGATGATGATAACTACC3'
IAA32	5'AGGGTGGTGGGTAATCG3'	5'CATAACCGTCGAGACCTATCAT3'
TCTP	5'ACACCCAAGCTCAGCGAAGAA3'	5'CATGCATACCCTCCCCAACAA3'
In vitro transcription/translation of TIR1/AFB tagged proteins		
3xFLAG	5'AGCTTAGACTACAAAGACCATGACGG5'GATCCGATATCACTGTACATCGTCATTGATTATAAGATCATGACATCGATTACCCCTGTAATCGATGTCATGATCTTATAAAGGATGACGATGACAAGTGATATCG3' ATCACCGTCATGGCTTTGTAGTCTA3'	
TIR1	5'GGGGACAACTTGTATACAAAAGTTG5GGGGACCACTTGTACAAGAAAGCT	GGGTATAATCCGTTAGTAGTAA3'
F: attB5	AAG	
attB2	CATGCAGAACGGAATAGC3'	
AFB1	5'GGGGACAACTTGTATACAAAAGTTG5'GGGGACCACTTGTACAAGAAAGC	
F: attB5	R: AAGCATGGGTCTCCGATTCCCACC3'	TGGGTACTTATGGCTAGATGTG3'
attB2		
AFB5	5'GGGGACAACTTGTATACAAAAGTTG5'GGGGACCACTTGTACAAGAAAGC	
F: attB5	R: AAGC ATGACACAAGATCGCTC3'	TGGGTATAAAATCGTGACGAACCTTG
attB2		
TIR1-3xFL	5'ATTGCGATCGCATGCAGAACGGAATA5'ACCGTTAAACTCACTGTACATCGT	
AG	GCC3'	CATCC3'
	(AsiSITIR1)	(FLAGPmeI)
AFB1-3xFL	5'ATTGCGATCGCATGGGTCTCCGATT(FLAGPmeI)	
AG	CC3'	
	(AsiSIAFB1)	
AFB2-3xFL	5'ACCGCGATCGCATGAATTATTCCCA(FLAGPmeI)	
AG	G3'	
	(AsiSIAFB2)	
6xHIS-	5'GCATCATCACCATCACCATATGTCTGC5'AGCTTGTAAACTCATTCAAAG	
ASK1	GAAGAAGATTGT3'	CCCATTGGTTCTC3'
	(HISASK1)	(ASK1PmeI)
6xHIS-	5'GTGTGCGATGCCATGCATCATCACC (ASK1PmeI)	
ASK1	ATCACCAT3'	
	(AsiSIHIS)	

Supplementary references

Hamant O, Heisler MG, Jonsson H, Krupinski P, Uyttewaal M, Bokov P, Corson F, Sahlin P, Boudaoud A, Meyerowitz EM, Couder Y, Traas J (2008) Developmental patterning by mechanical signals in *Arabidopsis*. *Science* **322**: 1650-1655.